Variation of Junction Breakdown Voltage by Charge Trapping*

ROLAND H. HAITZ†
Shockley Research Laboratory, Clevite Corporation, Semiconductor Division, Palo Alto, California
(Received 9 November 1964)

A variation of the avalanche breakdown voltage V_b resulting from charge trapping as predicted by Shockley was experimentally verified for silicon p-n junctions. The breakdown voltage of a p-n junction is determined by the space-charge density within the depletion layer, e.g., for the case of an n^+p step junction, by the density of ionized acceptors and ionized traps. Consequently, any variation in the amount of trapped charge resulting either from carrier capture or impact ionization during breakdown will lead to a corresponding variation of V_b. If the sign of the charge trapped during breakdown is such as to decrease the space-charge density, the space-charge layer widens and V_b is increased. If, however, the trapped charge increases the space-charge density, then the breakdown voltage is lowered and a "lock-on" mechanism prevents random on-off fluctuations. Both effects were observed in silicon p-n junctions at −196°C. A detailed analysis of this effect for the case of small uniform avalanche diodes with known dimensions allows the determination of trap density, integrated capture cross section for hot holes, and average capture time from the experimental results.

1. INTRODUCTION

THE avalanche breakdown voltage of an idealized p-n junction is determined by the space-charge density within the depletion layer. This space-charge density, in turn, is dominated in extrinsic crystal material by the density of such ionized donors and acceptors whose energy level is within a few kT of the conduction band and valence band, respectively. Such donors and acceptors can be considered to be completely ionized. In addition to these shallow donors and acceptors, the space-charge layer may also contain deep traps, which may be either neutral or ionized, depending on carrier capture and emission probabilities.

In a real p-n junction, the avalanche breakdown voltage is usually modified by crystal imperfections such as dislocations and precipitates. At such defects the breakdown voltage may be reduced locally to values considerably below the breakdown voltage of the surrounding uniform junction. Furthermore, the avalanche current passing through these highly localized breakdown centers—called microplasmas—fluctuates randomly between an on-state and an off-state.[1]

Shockley[2] tried to explain these random current fluctuations by a "lock-on" mechanism based on the presence of deep traps within the breakdown region. According to Shockley's model, impact ionization of deep traps by hot carriers may induce a space charge which has the opposite sign to the ionizing carriers. As a result, the space-charge density within the depletion layer should be increased, and the breakdown voltage should be decreased below its initial value. Refined experimental techniques led to a discrepancy between Shockley's model and experimental results. A better agreement experiment and theory was obtained for a mechanism proposed by McIntyre,[3] which explained the random current fluctuations without the need of deep traps within the space-charge layer.

In the meantime, Shockley's trap model has stimulated several investigations on avalanche breakdown.[4–6] In this paper, Shockley's model is the key to an understanding of important details of current fluctuations during avalanche breakdown. It is the subject of this paper to discuss the variation of the avalanche breakdown voltage V_b by trapping of space charge by deep traps. In Sec. 2, a detailed theoretical and experimental analysis of a breakdown voltage increase during breakdown is given. In Sec. 3, a breakdown voltage reduction is discussed briefly.

Haitz and Goetzberger[7] have recently found that microplasma breakdown and uniform avalanche breakdown are governed by essentially the same mechanism. Therefore, the term "avalanche breakdown" will be used for a general treatment of both cases.

2. INCREASE OF V_b BY CHARGE TRAPPING

2.1 Model

The statistics of carrier capture and emission by traps have already been discussed in several publications.[8,9] For use in the analysis of this paper, the Shockley-Read[8] method will be briefly reviewed. This method describes four basic processes, which are illustrated in Fig. 1: (1) electron emission, (2) hole emission, (3) electron capture, and (4) hole capture. E_t shall denote the trap energy level in the forbidden band, and E_c and E_v shall denote the lower edge of the conduction band and the upper edge of the valence band,

* Research supported by Contract DA49-196-ORD-1086, Harry Diamond Laboratories.
† Present address: Physics Research Laboratory, Texas Instruments, Inc., Dallas, Texas.
[1] K. C. McKay, Phys. Rev. **94**, 877 (1954).
[2] W. Shockley, Solid State Electron. **2**, 35 (1961).
[3] R. J. McIntyre, J. Appl. Phys. **32**, 983 (1961).
[4] R. H. Haitz, J. Appl. Phys. **35**, 1370 (1964).
[5] R. H. Haitz, A. Goetzberger, R. M. Scarlett, and W. Shockley, J. Appl. Phys. **34**, 1581 (1963).
[6] R. H. Haitz (to be published).
[7] R. H. Haitz and A. Goetzberger, Solid State Electron. **6**, 678 (1963).
[8] W. Shockley and W. T. Read, Jr., Phys. Rev. **87**, 835 (1952).
[9] R. N. Hall, Phys. Rev. **87**, 387 (1952).

respectively. The probability for the emission of an electron into the conduction band is determined by $E_n=E_c-E_t$, and the probability for the emission of a hole into the valence band by $E_p=E_t-E_v$. In the analysis, f_n represents the fraction of traps in the more negative state (e.g., ionized acceptors or neutral donors) and f_p the fraction in the more positive state (e.g., neutral acceptors or ionized donors). These quantities evidently satisfy the relation

$$f_n=1-f_p. \tag{1}$$

Under equilibrium conditions, f_n and f_p are simply the Fermi factors for the traps.

In their analysis, Shockley and Read use two emission constants e_n and e_p for electrons and holes, respectively. These two constants have the dimension of sec^{-1} and describe the rate at which a single trap emits electrons or holes. Two similar constants c_n and c_p with the dimension sec^{-1} describe the rate at which electrons and holes are captured by a trap. If v_n and v_p define the maximum drift velocities of electrons and holes in the high electric field of a p-n junction, and if σ_n and σ_p define the average capture cross sections for hot electrons and holes, then the capture constants c_n and c_p can be expressed as

$$c_n=v_n\sigma_n, \tag{2}$$

$$c_p=v_p\sigma_p. \tag{3}$$

If N_t denotes the trap density, then the rate for spontaneous emission of electrons and holes per unit volume is given by $e_nf_nN_t$ and $e_pf_pN_t$. Similarly, the capture rate for electrons and holes per unit volume is given by $nc_nf_pN_t$ and $pc_pf_nN_t$. Here, n and p are the customary symbols for the density of free electrons and holes. In the bulk material of a semiconductor, the mass-action law holds under equilibrium conditions

$$np=n_i^2, \tag{4}$$

where n_i denotes the intrinsic electron density. Equation (4) leads by the principle of detailed balance to the following relationship between the four emission and capture constants:

$$e_ne_p=n_i^2c_nc_p. \tag{5}$$

The investigations reported in this paper are dealing with traps within the high electric field of reverse biased p-n junctions. For such a case, Eqs. (4) and (5) are not valid because free carriers are swept out of the space-charge layer by the high field. In such a surrounding, with an extremely small density of free carriers, the traps have practically no chance to capture any carriers. Therefore, these traps can change their charge only by alternating emission of electrons and holes. An equilibrium will be reached such that the rates of electron and hole emission are equal:

$$e_nf_{n0}=e_pf_{p0}. \tag{6}$$

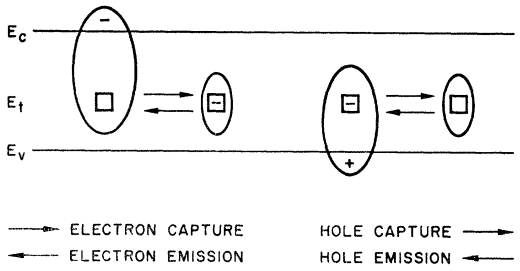

FIG. 1. Four basic processes of carrier recombination and generation at defect centers.

The subscript 0 of the Fermi factors refers to the steady-state condition for practically zero density of free carriers in the space-charge region.

Completely different steady-state conditions will be found if the junction is driven into avalanche breakdown. During avalanche breakdown, free carrier concentrations of the order of 10^{14} cm^{-3} to 10^{16} cm^{-3} are reached. Under such conditions, electron and hole capture by traps cannot be neglected. Similarly, electrons and holes can be knocked off from traps by hot carriers. Thus, the charge distribution of the traps during avalanche breakdown will be different from the distribution before breakdown. The steady-state condition during avalanche breakdown, which is reached after a short transition period, shall be characterized by the Fermi factors f_{n1} and $f_{p1}=1-f_{n1}$, the subscript 1 denoting the steady-state condition of avalanche breakdown.

For a quantitative analysis of these trapping effects, a simple field model of an n^+p step junction [Fig. 2(a)] is used. The space-charge layer of this junction having a maximum field E_m and a width W is divided into three different sections based on the simplifying assumption that secondary ionization takes place only in those parts of the junction where the electrical field exceeds a certain value E_i [Fig. 2(b)]. Only within this ionization region are both types of carriers present. At breakdown, the distribution of free carriers within the space-charge layer is shown schematically in Fig. 2(c).

For the case of an n^+p step junction, the field within the ionization region will be most sensitive to charge trapping within the lightly doped p region of the space charge layer. Under avalanche breakdown conditions, the main part of this p region contains only free holes flowing from the ionization region in Fig. 2(c) towards the p-type bulk. During this transition, the hot holes can change the charge distribution of traps in two ways: (1) Holes can be trapped, changing the charge state of traps by $+q$. (2) Hot holes can knock off either a positive or a negative charge from the traps leading to a charge change of either $-q$ or $+q$, respectively. A charge change of $+q$ decreases the space-charge density within the p region of the junction and results in an increased breakdown voltage $V_{b1}>V_{b0}$. Similarly, a negative charge change of the traps increases the space

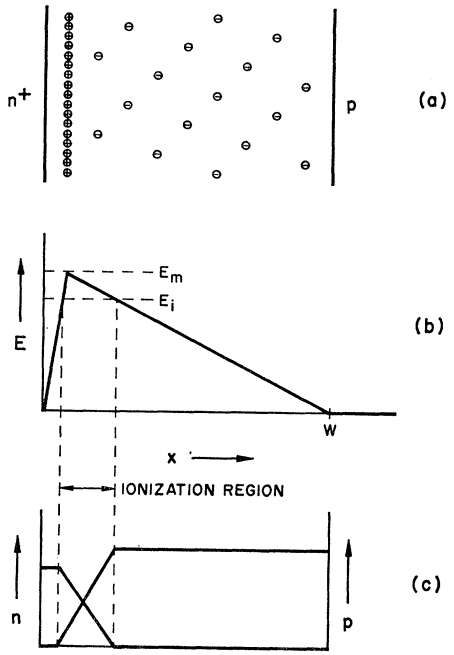

FIG. 2. Model of an n^+p step junction: (a) distribution of fixed charges within the depletion layer; (b) field distribution; (c) density of hot electrons and holes within the space-charge layer during avalanche breakdown.

charge density in the p region and results in a decrease of the breakdown voltage: $V_{b1}<V_{b0}$.

In the next paragraphs, an increase of the breakdown voltage due to a positive charge change is analyzed in detail. To simplify the discussion, it is assumed that the positive charge change is caused by hole trapping at negatively charged acceptor-type traps with a level in the lower half of the energy gap. This analysis will also hold for two other mechanisms which may cause a positive charge change: (1) for the case of hole trapping by neutral donor-type traps and (2) for the case that hot holes knock off electrons from neutral or negatively charged traps.

To investigate the influence of charge trapping during avalanche breakdown, it is necessary to estimate the charge distribution of the traps before breakdown. Equation (6) states that under steady-state conditions before breakdown the rate of electron emission is equal to the rate of hole emission. The emission coefficients e_n and e_p of Eq. (6) depend exponentially on the activation energies E_n and E_p, respectively. In a first approximation one can make the following assumption:

$$e_n/e_p=f_{p0}/f_{n0}\approx\exp[-(E_n-E_p)/kT]. \qquad (7)$$

In the case of an acceptor level in the lower half of the energy gap for which $E_n-E_p\gg kT$, one obtains from Eqs. (1) and (7):

$$f_{p0}\ll f_{n0}\approx 1. \qquad (8)$$

Equation (8) states that practically all traps are negatively charged under steady-state conditions before breakdown. This situation is illustrated in Figs. 3(a) and (b) for space charge and field distribution within the junction. E_{m0} and W_0 denote the maximum electric field and the junction width, respectively, before breakdown.

During avalanche breakdown, the charge distribution of the traps may be changed considerably due to the capture of holes by the negatively charged traps. These holes will be trapped for an average time τ_p before being

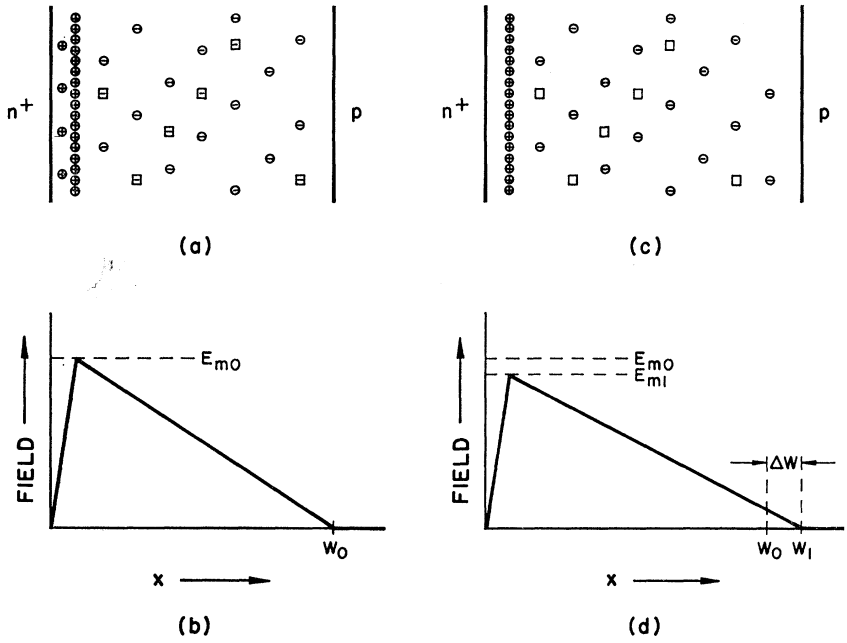

FIG. 3. The influence of charge trapping on the maximum field E_m: (a), (c) schematic distribution of fixed charges within the depletion layer before and during breakdown, respectively; (b), (d) field distribution before and during breakdown.

re-emitted. Under steady-state conditions, the capture rate must be equal to the emission rate for holes since both electron capture and emission are negligible:

$$pc_p f_{n1} = e_p f_{p1}. \tag{9}$$

A special case of this charge trapping process is given when

$$pc_p \gg e_p. \tag{10}$$

Under such steady-state conditions, one finds that practically all traps are filled with holes. The resulting Fermi factors during breakdown are then obtained from Eq. (9):

$$f_{n1} \ll f_{p1} \approx 1. \tag{11}$$

The space-charge distribution of the traps and the electric field during breakdown are illustrated in Figs. 3(c) and (d). E_{m1} denotes the maximum field and W_1 the junction width during breakdown.

Comparing Eq. (8) with Eq. (11), one finds that practically all traps change their charge from $-q$ to neutral. The exponential transition from the pre-breakdown charge distribution to the charge distribution during breakdown is determined by a time constant θ_p which is given by

$$\theta_p = 1/pc_p. \tag{12}$$

θ_p is the average time for the negatively charged traps to capture a hole at a density of p holes per unit volume. From Eqs. (3) and (12), it is obvious that θ_p is inversely proportional to free-hole density p and hole-capture cross section σ_p. Since the hole density p and the maximum hole drift velocity v_p are known, the integrated capture cross section for hot holes can be calculated from experimental values of θ_p:

$$\sigma_p = 1/p\theta_p v_p. \tag{13}$$

After avalanche breakdown has ceased, the carriers will be trapped for an average time τ_p before being re-emitted. The charge distribution of the traps which is characterized by the Fermi factor $f_{p1} = 1 - f_{n1} \approx 1$, will change exponentially to the pre-breakdown steady-state distribution characterized by $f_{n0} = 1 - f_{p0} \approx 1$. This exponential change of the charge distribution is determined by the time constant τ_p.

For a quantitative analysis of the variation of junction breakdown voltage by charge trapping, it is necessary to relate the hypothetical model outlined above to experimentally measurable quantities. Such a relation is discussed with reference to Fig. 4. An increase of the extrapolated breakdown voltage[10] from a pre-breakdown value V_{b0} to a value V_{b1} during breakdown is illustrated in the left part of Fig. 4. Diode current is plotted as a function of voltage. The diode current corresponding to the charge distribution of the traps before breakdown is I_0. The current corresponding

[10] For the definition of the extrapolated breakdown voltage see R. H. Haitz (Ref. 4).

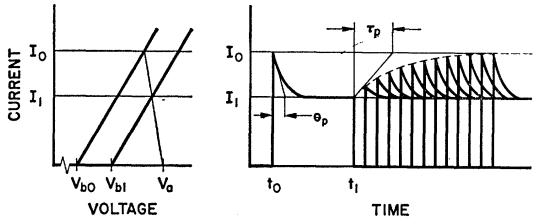

FIG. 4. Shape of the current pulses during avalanche breakdown explained by an increase of the breakdown voltage from V_{b0} to V_{b1}.

to the steady-state charge distribution during breakdown is denoted by I_1. Both currents are given by the intersection of the load line (originating at the applied voltage V_a) with the corresponding V–I characteristic. If R_s and R_L denote diode and load impedance, respectively, then the variation in breakdown voltage is given by

$$\Delta V_b = V_{b1} - V_{b0} = (R_s + R_L)(I_0 - I_1). \tag{14}$$

The avalanche current as a function of time is illustrated in the right-hand section of Fig. 4. Suppose the avalanche is triggered by a carrier entering the breakdown region at time t_0. Within a short time determined by the diode series resistance R_s and the total shunting capacitance C, the current will rise to I_0. Owing to this current, the space-charge layer is flooded with carriers, which are distributed according to Fig. 2(c). Holes will be trapped, resulting in an increase of the breakdown voltage from V_{b0} to V_{b1}. As a result, the diode current $I(t-t_0)$ will gradually drop from I_0 to a new steady-state current I_1, according to

$$I(t-t_0) = I_1 + (I_0 - I_1) \exp[-(t-t_0)/\theta_p]. \tag{15}$$

The recovery of the junction from V_{b0} to V_{b1} is also discussed with reference to Fig. 4. Suppose the avalanche discharge is interrupted at time t_1. The emission of trapped holes will take on the average a time τ_p. If the avalanche is triggered again at a time t for which $t-t_1$ is of the order of τ_p or less, than a considerable fraction of traps will still be occupied by holes, and the breakdown voltage will not completely recover to its pre-breakdown value V_{b0}. As a result, the current $I_0'(t-t_1)$ at the beginning of a discharge will be less than I_0 as illustrated in Fig. 4. The current $I_0'(t-t_1)$ is given by

$$I_0'(t-t_1) = I_0 - (I_0 - I_1) \exp[-(t-t_1)/\tau_p]. \tag{16}$$

The effective trap density can be determined from experimental values of $I_0 - I_1$. For the case of acceptor-type traps in the lower half of the energy gap, practically all traps are negatively charged before breakdown. It has already been mentioned above that practically all traps will become neutral during breakdown if $pc_p \gg e_p$. For this special case, the increase in breakdown voltage ΔV_b should become independent of the hole density p

and, therefore, of current I_0. The trap density N_t can be estimated from the following experimentally determined[11] relation between the acceptor concentration N_a of the starting p material and the breakdown voltage V_b of shallow diffused n^+p step junctions:

$$N_a = 1.2\times 10^{19} V_b^{-2.35}. \tag{17}$$

The effective trap concentration N_t is obtained from the derivative of Eq. (17) with respect to V_b:

$$N_t = 2.8\times 10^{19} V_b^{-3.35} \Delta V_b. \tag{18}$$

In summarizing the model outlined above, one can say that the current spike discussed with reference to Fig. 4 has three essential features:

(1) The spike amplitude $I_0 - I_1$, and, consequently, the increase in breakdown voltage ΔV_b are constant and independent of I_0.

(2) The time constant θ_p, which determines the current decay from I_0 to I_1, is a function which decreases inversely with p and, consequently, with I_0 [see Eq. (12)].

(3) The spike amplitude of a closely following avalanche pulse increases exponentially with the preceding off-time [Eq. (16)].

These three characteristic features of the current spike will be studied in the next section in order to determine the validity of the model.

2.2 Experimental Results and Discussion

In order to analyze the experimental results in terms of the theoretical model of Sec. 2.1, it is necessary to determine the hole density p within the space-charge layer during avalanche breakdown. Straightforward calculation leads to the following relation between p and the current I_0 at the beginning of an avalanche discharge:

$$p = I_0/qv_pA\,, \tag{19}$$

where A denotes the junction area over which avalanche breakdown occurs.

Since the accuracy of p depends mainly on the accuracy of A, it is obvious that specially designed microplasma free junctions have to be used for these investigations. Furthermore, the breakdown area A has to be small in order to obtain high hole concentrations at relatively small currents. Small avalanche currents of a few milliamperes or less are required in order to avoid thermal effects which may interfere with the measurements. A guard ring design was chosen with a 17μ diam of the n^+p breakdown junction.[5,7] From studies of both V-I characteristic and light emission, it was found that the junctions were microplasma free and that avalanche breakdown occurred uniformly over the entire breakdown area.

[11] R. H. Haitz, Second Annual Scientific Report on Contract No. DA49-186-ORD-1086, Harry Diamond Laboratories, Washington, D. C., 1964, p. 79 (unpublished).

In order to study current spikes like those shown in Fig. 4, the following experimental arrangement was chosen. The diode was reverse biased from a dc voltage source through a 100-Ω current viewing resistor. The applied dc bias was slightly less than the breakdown voltage V_{b0}. At the time t_0, a rectangular voltage pulse of width $t_1 - t_0 = 1$ msec was superimposed onto the dc voltage. The rise time of the voltage pulse was approximately 10^{-7} sec. The polarity of the voltage pulse was such that the reverse bias across the junction was increased. As soon as the total applied voltage exceeded the breakdown voltage V_{b0} at time t_0, an avalanche discharge was triggered.[12] The discharge was interrupted at time t_1 by lowering the total applied voltage to a value below V_{b0}. The voltage drop across the 100-Ω current viewing resistor was displayed on a cathode-ray tube as a function of time. In keeping with the model of Sec. 2, current pulses as illustrated in Fig. 4 were observed if the diode was cooled to 77°K. The reason for this low operating temperature is discussed below.

The three characteristic features of the current spike described at the end of Sec. 2.1 were investigated experimentally. Variations of I_0 from 200 μA to 10 mA left the spike amplitude $I_0 - I_1 = 230$ μA unchanged, as predicted in Sec. 2.1. The sensitivity of the experiment was high enough to detect a 10% change of the spike amplitude $I_0 - I_1$. It is therefore concluded that $I_0 - I_1$ is independent of I_0.

The inverse dependence of θ_p on I_0 as predicted by Eq. (12) is studied by plotting the rate of current change $(dI/dt)_{t_0}$ at the beginning of an avalanche discharge as a function of I_0. Since $-(dI/dt)_{t_0}$ is inversely proportional to θ_p, one expects a linear dependence of $(dI/dt)_{t_0}$ on I_0. The measured dependence of $(dI/dt)_{t_0}$ on I_0 is plotted in Fig. 5(a). The expected linear relationship is observed.

The exponential recovery of the breakdown voltage from V_{b1} to V_{b0} was studied by reducing the time between successive avalanche discharges to the order of τ_p or less. The function $I_0 - I_0'$ was measured for various values of the preceding off-time $t - t_1$. The experimental results are plotted in Fig. 5(b). The exponential dependence expected from Eq. (16) is observed over one order of magnitude in $I_0 - I_0'$.

A quantitative evaluation of the experimental data is the subject of this paragraph. A series resistance of $R_s = 770$ Ω, a load impedance of $R_L = 100$ Ω, and an experimental value of $I_0 - I_1 = 230$ μA lead, according to Eq. (14), to a variation in breakdown voltage of $\Delta V_b = 200$ mV. With $V_b = 32$ V, the trap density N_t is calculated from Eq. (18) to be $N_t = 5\times 10^{14}$ cm^{-3}.

[12] An applied voltage V_a larger than V_{b0} is not sufficient for avalanche breakdown to occur. In addition, a free carrier is required to trigger the discharge. In order to avoid any breakdown delays of more than 1 μsec, the junction was illuminated weakly. It could be shown that this illumination did not interfere with the effects studied.

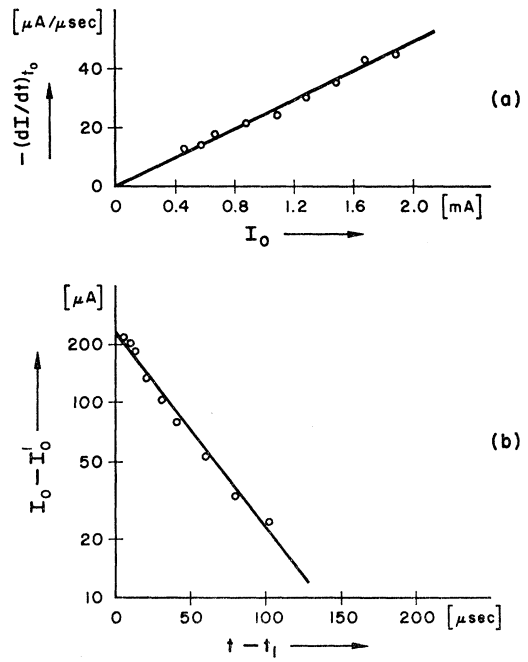

FIG. 5. Experimental results: (a) rate of current change at the beginning of a pulse as a function of I_0; (b) exponential recovery of the spike amplitude as a function of the preceding off-time $t-t_1$.

From the experimental results of Fig. 5(a), one obtains $\theta_p=7.2$ μsec at $I_0=1$ mA. The hole density p for $I_0=1$ mA and a 17 μ diam of the breakdown region is calculated from Eq. (19) to be $p=4\times10^{14}$ cm^{-3}. For these calculations, a maximum drift velocity for holes of $v_p=6\times10^6$ cm/sec is used.[13] For the calculation of σ_p, the value of v_p is not critical, because the occurrence of v_p in Eq. (19) cancels that in Eq. (13). The effective cross section for hot holes is then obtained from Eq. (13) to be $\sigma_p=5\times10^{-17}$ cm^2. The average capture time for holes at a temperature of 77°K is readily calculated from the slope of the experimental curve in Fig. 5(b) to be $\tau_p=45$ μsec.

From the model of Sec. 2.1, it can be concluded that a variation of the junction breakdown voltage by charge trapping is only possible if τ_p is of the order of θ_p or larger. In order to keep practically all traps filled with holes during breakdown, it is necessary that $\tau_p\gg\theta_p$. For the diodes under investigation, a ratio of $\tau_p/\theta_p=6.3$ was found at a temperature of 77°K, resulting in a spike amplitude, which is independent of I_0. At higher temperatures, e.g., at room temperature, τ_p will become much less than θ_p. As a consequence, no variation or only a small variation of the breakdown voltage should be observed. Indeed, only a small current spike was found at room temperature, which increases with I_0. This dependence on I_0 is in agreement with the model of Sec. 2.1. For the case that $pc_p\ll e_p$, one obtains from Eq. (9):

$$f_{p1}\approx pc_p/e_p. \tag{20}$$

Since ΔV_b increases in proportion to $f_{p1}-f_{p0}\approx f_{p1}$, it is evident that the small current spike at room temperature should increase with current I_0.

An interesting conclusion concerning the trapping model of Sec. 2 can be drawn from the experimental results of Fig. 5(b). Within the experimental accuracy, the quantity I_0-I_0' [see Eq. (16)] is determined by a single time constant τ_p over a range of one order of magnitude. From this observation it can be concluded that the variation of the breakdown voltage is caused by a single kind of traps. It can be further concluded that the traps change their charge by one elementary unit q. A charge change by $2q$ would lead to two different recovery-time constants.

Similar current spikes have also been observed occasionally during noise studies of diodes containing microplasmas. However, such microplasma diodes are not suitable for a detailed investigation of the current spikes because of several shortcomings arising from imperfect junctions. For instance, the cross section of microplasmas is not well known.[5] Further, the effect is not reproducible from one microplasma to another, because the formation of microplasmas is uncontrolled and due to imperfections in the crystal or due to surface defects. Another difficulty arises from the presence of a large number of microplasmas on every large-area avalanche diode. Breakdown of several microplasmas usually inerferes, if breakdown studies of a single microplasma are carried out over a larger current range. In spite of such experimental difficulties, it can be said that the observations agree with those described for the case of small microplasma free diodes: The spike amplitude is independent of current, the time constant describing the current decay decreases with current, and the spike amplitude recovers in a way described by Eq. (16).

It should also be mentioned that, for the case of microplasmas, current spikes have been occasionally observed even at room temperature, but not as often as at low temperatures. Such observations of current spikes are not surprising, since it is known that trapping centers contribute considerably to the noise pulse rate of microplasmas.[6] Earlier in this section, it was mentioned that a variation of the breakdown voltage can be observed only if $\tau_p\geq\theta_p$. For the case that θ_p is very small because of a large capture cross section for holes or because of large carrier densities, it may be possible to observe a variation of V_b even at room temperature. The same considerations hold also for large values of τ_p resulting from high activation energies of the order of half the band gap.

As already mentioned in Sec. 2.1, it cannot be determined from the model which of four possible mechanisms causes the positive charge change during breakdown: capture of hot holes by negatively charged acceptor-type or by neutral donor-type traps, or

[13] J. B. Gunn, Progr. Semiconductors 2, 211 (1957).

impact ionization of negatively charged acceptor-type traps or of neutral donor-type traps by hot holes. From the experimentally determined cross section of $\sigma_p = 5 \times 10^{-17}$ cm^2, it is supposed that the observed interaction consists either in a trapping or impact ionization process between hot holes and negatively charged acceptor-type traps. For an interaction between hot holes and neutral donor-type traps, a much smaller cross section is expected.

It should be mentioned that current spikes similar to those of Fig. 4 have also been described by McIntyre.[3] McIntyre explained his observations as a thermal effect caused by high-power dissipation within the reverse biased p-n junction. The temperature rise during an avalanche pulse increases the breakdown voltage and simultaneously decreases the current to a lower value. For the observations reported in this publication, such an explanation is excluded, since the spike amplitude $I_0 - I_1$ is independent of I_0. From thermal effects, one expects a linear dependence of spike amplitude on I_0, since $\Delta V_b/V_b \ll \Delta I/I_0$. There is also another observation which agrees with a trapping mechanism and contradicts a thermal effect. After a heat treatment of the diodes at 400°C for a few minutes, the current spike disappears almost completely. Such an effect can be explained by annealing of trapping centers. It is very unlikely that the thermal resistance of an unmounted diode should be affected by a short heat treatment.

3. REDUCTION OF V_b BY CHARGE TRAPPING

In Sec. 2, only the trapping of positive charges within the space-charge layer of n^+p step junctions has been discussed. Similar considerations would also apply to negative charge trapping leading to a reduction of the breakdown voltage. However, the result of negative charge trapping would not be a current spike, as discussed with reference to Fig. 4, but an increase of current with time causing a "lock-on" mechanism proposed by Shockley.[2]

Before describing the experimental results, a brief discussion of the lock-on mechanism resulting from a breakdown voltage reduction will be given. Suppose the breakdown voltage before charge trapping is V_{b0} and during breakdown $V_{b1} < V_{b0}$. The corresponding current voltage characteristics are shown schematically in Fig. 6. If at time t_0 a voltage V_a is applied, the diode will turn on to a current I_0 given by the intersection of prebreakdown characteristic and load line, provided a trigger carrier is also available at t_0. The avalanche current I_0 starts to induce a negative charge change resulting in a decreasing breakdown voltage with time. Simultaneously, the diode current increases until the breakdown voltage drops to the steady-state value V_{b1}. The corresponding steady-state avalanche current is denoted by I_1.[14] If $V_{b0} - V_{b1}$ is of the order of a volt, then the current I_1 will be large enough to sustain avalanche breakdown.[4] Such a lock-on mechanism

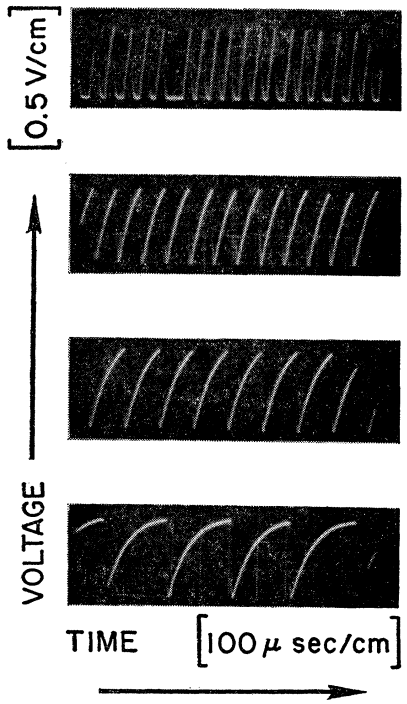

FIG. 7. Relaxation oscillations of a microplasma for the case that the breakdown voltage is reduced during breakdown by trapping of space charge; the average current passing through the microplasma increases from bottom to top.

prevents the turn-off of the avalanche discharge. As a result, no random current fluctuations are observed on such a diode. In order to interrupt the discharge, V_a has to be lowered to a value close to V_{b1}.

Such a diode exhibiting a reduction of V_b by charge trapping should behave similarly to a gas discharge with an ignition voltage slightly larger than V_{b0} and a sustaining voltage slightly larger than V_{b1}. If this model is correct, then relaxation oscillations with an amplitude of approximately $V_{b0} - V_{b1}$ should be observed in a high-impedance circuit. A photograph of

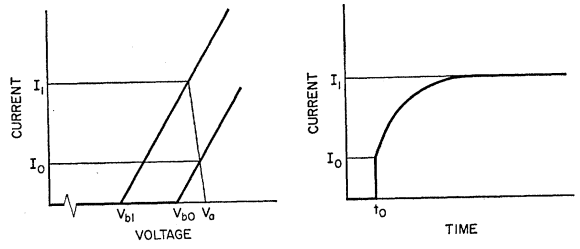

FIG. 6. Current as a function of time during avalanche breakdown explained by a reduction of the breakdown voltage from V_{b0} to V_{b1}.

[14] For the experimental diode described in this section, the transition from I_0 to I_1 was faster than the rise time of the scope, i.e., faster than 50 nsec.

such relaxation oscillations observed at 77°K on a large diode (diameter = 600 μ) containing microplasmas is shown in Fig. 7. The amplitude of these oscillations is nearly constant. Its variation with applied voltage will be discussed later in this section. The oscillation frequency depends on applied voltage and circuit, as expected from a gas discharge model.

Further conclusions about the oscillation mechanism can be obtained from the dc current-voltage characteristic during breakdown shown in Fig. 8 (open circles). The breakdown voltages $V_{b0}=22.0$ V and $V_{b1}=19.9$ V are indicated. The V-I characteristic could be measured only up to approximately 21 V. At that voltage the breakdown of several microplasmas exhibiting the usual microplasma noise interfered with the measurements. The constant series resistance R_s of the diode is 11 kΩ, leading to the suggestion that breakdown is restricted to an area of the order of 1 μ in diameter (typical microplasma diameter). Furthermore, it is found that the discharge is interrupted if dc current is lowered to approximately 20 μA. Such a turn-off current is also typical for microplasmas with a series resistance of the order of 11 kΩ. It is, therefore, concluded that a microplasma whose breakdown voltage is reduced from V_{b0} to V_{b1} by charge trapping is causing the relaxation oscillations of Fig. 7.

From the voltage difference $V_{b0}-V_{b1}$, an oscillation amplitude of the order of 2 V is expected. The observed amplitude, however, is only 1.4 V and decreases slightly with repetition rate. These two observations lead to the suggestion that not all trapping centers will emit the electrons between successive discharges. As a result, the oscillation amplitude is less than $V_{b0}-V_{b1}$.

On the same diode, another microplasma exhibiting a breakdown voltage reduction during breakdown is found (closed circles in Fig. 8). The ignition voltage is 22.1 V, slightly larger than that for the microplasma described above. The extrapolated voltage V_{b1} during breakdown is approximately 17 V. The series resistance is 48 kΩ. This second microplasma does not oscillate, because its ignition voltage is larger than V_{b0} of the first microplasma. The second microplasma can be switched on only in a low-impedance circuit by increasing the voltage across the diode terminals to 22.1 V. Reducing the voltage to approximately 19.5 V, the first microplasma can be turned off, and the V-I characteristic of the second microplasma (closed circles) can be measured separately.

At the end of this section, it will be necessary to review the definition of the extrapolated breakdown

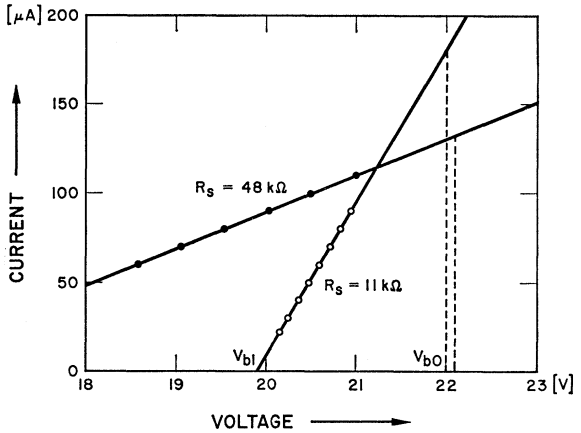

FIG. 8. Current voltage characteristic of two microplasmas exhibiting a breakdown voltage reduction during breakdown by charge trapping.

voltage given by Haitz.[5] There it was found that the two breakdown voltages V_{bm} and V_{bi}, which were obtained by exptrapolating the multiplication characteristic ($1/M$ versus V) and the current-voltage characteristic, respectively, are equal within the limits of the experimental error. For the case of charge trapping, this condition will no longer hold. V_{bi} will then be equal to V_{b1}, and V_{bm} will be equal to V_{b0}, provided that the photocurrent injected to study carrier multiplication is so small that charge trapping is negligible. The variation in breakdown voltage by charge trapping can be defined as

$$\Delta V_b = V_{b1}-V_{b0}=V_{bi}-V_{bm}. \tag{21}$$

For the case that charge trapping during breakdown is negligible, then $V_{bi}=V_{bm}$ and $\Delta V_b=0$.

4. CONCLUSION

A variation of the avalanche breakdown voltage resulting from charge trapping during breakdown is experimentally verified for silicon p-n junctions. A quantitative analysis of this effect allows the determination of trap density, integrated capture cross section for hot holes, and average trapping time from simple experimental results.

ACKNOWLEDGMENT

The author is greatly indebted to Dr. W. Shockley for his continuous interest and for many stimulating discussions during the course of this work.

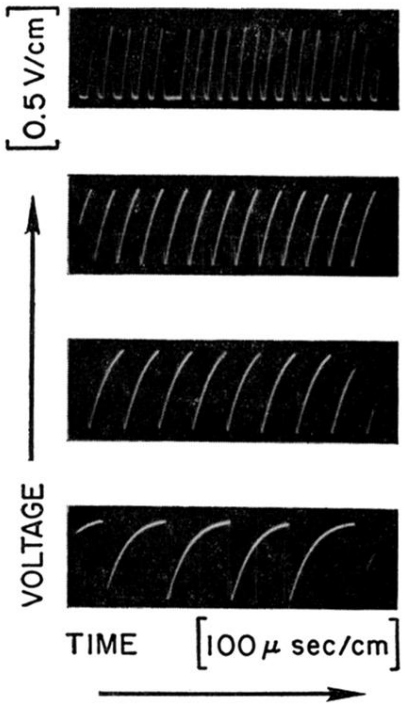

FIG. 7. Relaxation oscillations of a microplasma for the case that the breakdown voltage is reduced during breakdown by trapping of space charge; the average current passing through the microplasma increases from bottom to top.